Int. J. Electrochem. Sci., 7 **(2012)** 11734 - 11744

International Journal of
ELECTROCHEMICAL
SCIENCE
www.electrochemsci.org

Incorporation of Multi-Walled Carbon Nanotubes in ZnO for Dye Sensitized Solar Cells

Alagar Ramar[2], *Thiagarajan Soundappan*[1], *Shen-Ming Chen*[1,*], *Muniyandi Rajkumar* [1], *Saraswathi Ramiah*[1]

[1] Electroanalysis and Bioelectrochemistry Lab, Department of Chemical Engineering and Biotechnology, National Taipei University of Technology, No.1, Section 3, Chung-Hsiao East Road, Taipei 106.Taiwan (ROC).
[2] Department of Materials Science, School of Chemistry, Madurai Kamaraj University,Madurai-625 021,Tamil Nadu, India.
[*]E-mail: smchen78@ms15.hinet.net

Received: 30 October 2012 / *Accepted:* 18 November 2012 / *Published:* 1 December 2012

Dye-sensitized solar cells (DSSCs) based on ZnO/multi-walled carbon nanotube (MWCNT) nanocomposite films are prepared by mechanical grinding and spin coating method. As prepared nanocomposite films are further characterized by scanning electron microscopy (SEM), UV–vis absorption and impedance spectroscopy. The photoelectric performances of the DSSCs based on ZnO/MWCNT nanocomposite film electrodes with various concentrations (from 0.1 wt % to 0.5 wt %) are compared. The power conversion efficiency of MWCNT nanocomposite films are increasing up to 0.3 wt % while the excess loadings of MWCNT significantly reduces their performance. The optimum concentration of MWCNTs in ZnO for the best performance in DSSCs is found to be 0.3 wt %. The reason for this increment is that MWCNTs enhance the transport of electrons from the film to ITO substrate while for the decrease in the efficiency at higher concentrations (MWCNT) is due to light shielding effect of the denser composite, respectively.

Keywords: Dye sensitized solar cells; ZnO; ZnO/CNT; nanocomposite; N719 dye, electrochemistry.

1. INTRODUCTION

In recent years ZnO has been used in DSSCs more than TiO_2 which has been attributed to the relative ease of synthesizing highly crystalline ZnO (wurtzite form) with a variety of morphologies ZnO has a similar bandgap (3.2-3.3 eV) and conduction band edge to that of anatase TiO_2. The electronic mobility of ZnO is also higher than that of TiO_2 which could favor the electron transport [1-5]. Carbon nanomaterials like fullerenes, carbon nanotubes and graphene are currently being

intensively investigated in solar cell applications due to their unique electrical properties, large specific surface area, extraordinary chemical and mechanical stability [6,7]. Incorporation of the carbon nanomaterials into the matrix of the photoanode enables the improvement of the performance of absorbing layers by enhancing the light absorption and electron transport in the semiconducting nanostructured film [8, 9]. Especially, one dimensional carbon nanotubes have a large electron-storage capacity (one electron for every 32 carbon atoms) and exhibit metallic conductivity similar to metals [10]. Incorporation of carbon nanotubes in TiO_2 films as photoanode resulted in improving the efficiency by improved charge transfer, efficient charge collection [11], reducing the electrolyte/electrode interfacial resistance, lowering the recombination, enhances the charge transport[12] and improves interconnectivity of TiO_2 [13]. However only a few reports have been found in the literature where MWCNTs are used along with ZnO films in DSSCs. For example, vertically aligned carbon nanotubes improves the efficiency of ZnO based DSSCs [14]. Next the low temperature production of ZnO nanoparticles on a single-walled carbon nanotube stamped DSSCs with ionic liquid showed promising photocurrent [15]. To the best of our knowledge, those reports which are associated with the coating of ZnO thin films on a MWCNT coated thin films while no report was found which deals with the addition of MWCNTs into the ZnO matrix. In this study, we have incorporated different amount of acid treated multi-walled carbon nanotubes into nano ZnO by mechanical mixing to form ZnO/MWCNT composite films. The influence of different amounts of MWCNT with terminal-COOH groups [16] in ZnO matrix and the overall properties of DSSCs were studied. The experimental results suggested that MWCNT can reduce charge recombination and increases the J_{sc} to some extent and thus improves the conversion efficiency of the DSSCs, respectively.

2. MATERIALS AND METHODS

2.1. Materials

ZnO (< 100 nm), multi-walled carbon nanotube (MWCNT), fullerene (C_{60}, 99.5%), acetyl acetone, N719 dye, 4-*tert*-butylpyridine (TBP), Triton X-100 solution and polyethylene glycol (PEG_{20000}) were purchased from Sigma-Aldrich (USA). Commercial graphene (8 nm flakes) was purchased from Uni Region Bio-Tech. The MWCNT was oxidized in a concentrated 3:1 v/v acid mixture of H_2SO_4/HNO_3 under ultrasonication for 24 h at 50–60º C to produce MWCNT with terminal-COOH groups [16]. It is expected that the acid-treated MWCNTs would have good contact with the ZnO nanoparticles than the untreated one. Indium tin oxide (ITO) (12 Ω/cm^2) was purchased from Merck Display Technologies (MDT) Ltd (Taiwan). Lithium iodide (AR) and iodine (AR) were obtained from Wako (Japan). Surlyn films (60 μm thick) were purchased from Solaronix S.A., Aubonne, (Switzerland).

2.2. Preparation of ZnO/MWCNT electrodes

The ZnO/MWCNT composite as photoanodes were prepared by following the previous report [12]. ZnO nanopowder (2.4 g), PEG_{20000} (0.6 g) (to break up the aggregate into a dispersed paste), various amount (0.1 to 0.5 wt.%) of acid-treated MWCNTs, acetylacetonate (100 μL) (to extend the solidification time of the paste in the solution form) were grounded in an agate mortar with 14 mL deionized water for 30 minutes. Then 50 μL of TritonX-100 surfactant was added to facilitate the spreading of the colloid on the substrate. Finally it was transferred to a culture tube and stirred for one hour. Before fabricating ZnO/MWCNT composite films, the ITO substrates were ultrasonically cleaned sequentially in Triton X-100, acetone, ethanol and in water for thirty minutes and dried in an oven at 80ºC. This colloidal solution was spin coated on ITO surface (50 μL) 1000 rpm for 5 sec and 2000 rpm for 15 sec and annealed at 410ºC for 30 minutes. This process was repeated to three times to obtain the optimized thickness. After annealing, the film coated ITO substrates were cooled to 80ºC for dye sensitization. Further the annealed films were immersed for two and half hours in a 0.5 mM ethanol solution of N719 dye in a closed box. Finally the electrodes were washed with ethanol to remove surfeit dye from the surface and dried at room temperature.

2.3. Cell assembly of DSSCs

Cathode was prepared by spin coating the solution of 5 mM K_2PtCl_6 in isopropyl alcohol on a 0.25 cm^2 sputtered Pt and annealed at 385ºC for five minutes. The DSSC was fabricated by sealing the dye-sensitized ZnO photo-anode and Pt cathode with 60 μm hot melt sealing foil (surlyn film) which also served as a spacer. The whole setup was heated to 100ºC with 15 $Kgcm^{-2}$ pressure on the hot-press machine. The liquid electrolyte was composed of 0.3 M 4-*tert*-butylpyridine (TBP), 0.5 M LiI , and 0.05 M I_2 in acetonitrile. The DSSC cell (active area 0.25 cm^2) was completed upon the injection of the electrolyte into the cell.

2.4. Instruments and measurements

UV–visible spectra were obtained using Hitachi U-3300 spectrophotometer (Japan). The amount of adsorbed dye was determined by desorbing the dye from ZnO and carbon nanocomposite films (sensitized for 2 hrs) by soaking in a 1 mM KOH solution. The desorbed dye solution was further analyzed using UV-vis spectroscopy. Field emission scanning electron microscope (FE-SEM) images were recorded using a HITACHI S-4700 (Japan). The photovoltaic behaviors were measured by using a digital source meter (Keithley Instruments Inc., Model 2400) under an illumination of a solar simulator at one sun (AM 1.5, 100 mW/cm^2). The photoelectric conversion efficiency (η) and fill factor (FF) were calculated according to the following equations:

$$\eta\ (\%) = [(J_{sc} \times V_{oc} \times FF)/P_{in}] \times 100$$

$$FF = (J_{max} \times V_{max})/(J_{sc} \times V_{oc})$$

Where J_{sc} is the short-circuit current density, V_{oc} is the open circuit voltage, P_{in} is the incident light power and J_{max} and V_{max} are the photocurrent density and photovoltage at maximum power output (P_{max}). The electrochemical impedance spectra (EIS) were performed with a ZAHNER impedance analyzer (Germany) in a two-electrode configuration under illumination with at one sun (AM 1.5, 100 mW/cm^2). The measurements were carried out by applying bias of the open circuit voltage (V_{oc}) and recorded over a frequency range of 100 mHz to 100 kHz with ac amplitude of 10 mV.

3. RESULTS AND DISCUSSION

3.1. Optimizing the thickness of ZnO/MWCNT composite film

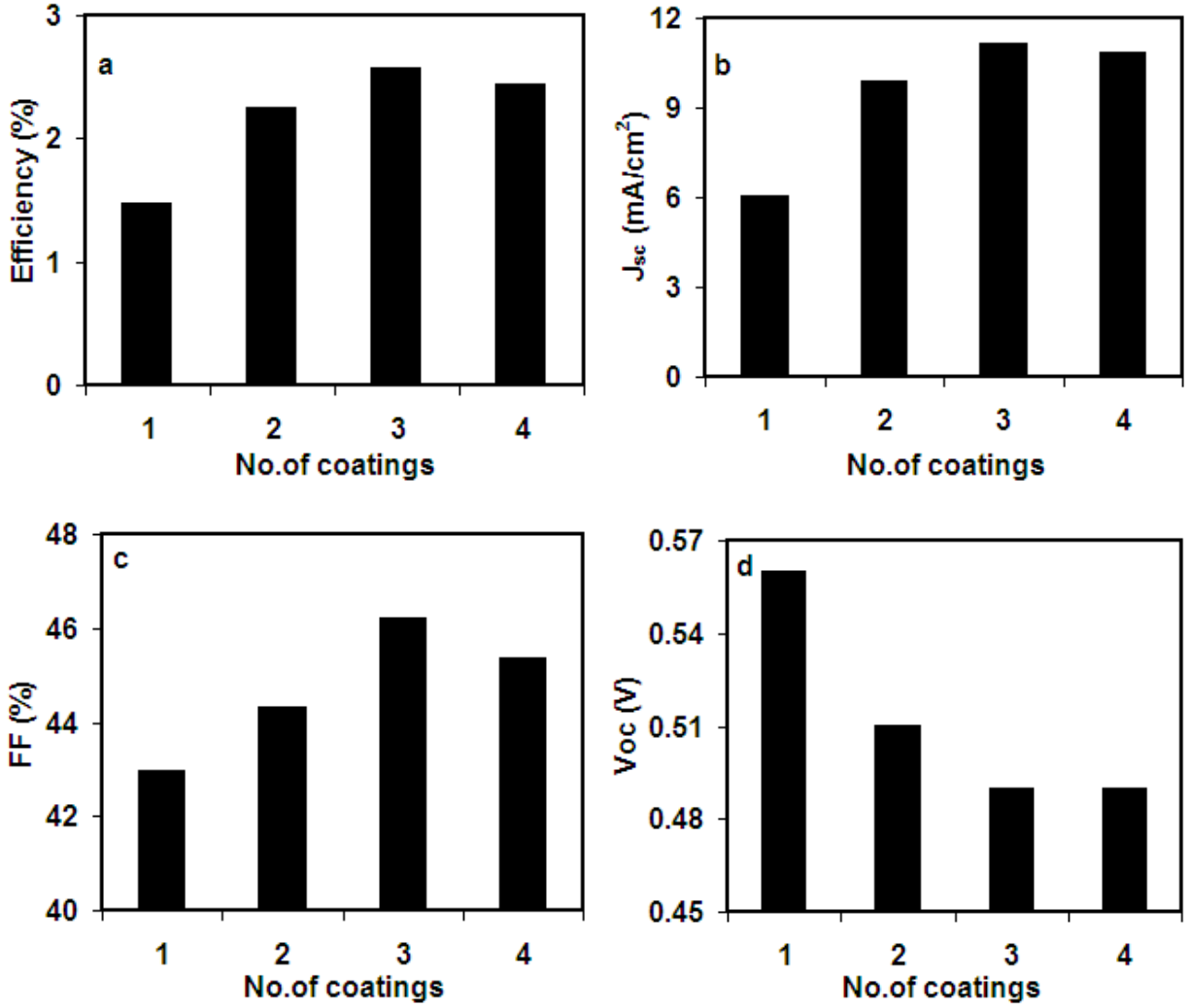

Figure 1. Photovoltaic characteristic parameters for the DSSC cells with various number of coatings of ZnO/MWCNT composite a) efficiency b) short circuit current density c) fill factor d) open circuit voltage.

In order to understand the role of MWCNTs in the composite film, at first the thickness of the composite films was optimized with the number of coatings. The DSSCs of ZnO/MWCNT blends show linear increase in short circuit current density, fill factor and efficiencies with increase in thickness up to three coating and then decrease slightly as shown in Figure. 1a-c, respectively. However it shows decrease in open circuit voltage upto three coating and thereafter no change with further increase in thickness (Figure. 1d). The efficiency, fill factor and short-circuit current density are maximum at three layers but open-circuit voltage is the minimum. At low output voltage, the intrinsic one dimensional carbon nanotubes facilitates the electron transport easily. At the same time, at the increasing voltage of cell, the energy dissipation increases significantly and MWCNTs slowly lose the role of electron transport channels [17]. Therefore, the thickness was optimized to three layers and it was measured as 65 μm, respectively.

3.2. Effect of dye sensitization

Table 1. Photovoltaic parameters of DSSCs based on ZnO/MWCNT composite films with different dye immersion times

Time (hrs)	J_{sc} (mA/cm^2)	V_{oc} (V)	FF (%)	η (%)
0.30	12.06	0.45	49.81	2.15
1	11.88	0.46	48.14	2.66
1.30	11.61	0.47	47.55	2.60
2	11.85	0.48	48.76	2.77
2.30	11.05	0.48	44.76	2.41
5	10.80	0.49	44.80	2.38
10	7.86	0.51	45.05	1.83
15	8.29	0.51	46.41	1.98
20	7.84	0.51	45.35	1.89
24	8.17	0.52	46.66	1.87

Dye sensitization process time is the important parameter to increase the overall performance of the DSSC. Table 1 shows the photovoltaic parameters of the DSSCs based on ZnO/MWCNT nanocomposite with the different immersion times. The dye immersion time have been varied from 0.30, 1, 1.30, 2, 2.30, 5, 10, 15, 20 and 24 hours. The ZnO/MWCNT nanocomposite shows maximum performance at the sensitized time of two hours and then decreases accordingly with the increasing time. Here the decrease in the efficiency (η) after 2 hours may be due to excessive dye which has been absorbed into the surface of the ZnO nanostructures. Further the excessive dye absorption could cause the Zn^{2+} ions of the outer layer of the ZnO nanostructures to dissolve into the solution by the acidic carboxylate groups of the N719 dye molecule, and subsequently will form a Zn^{2+}- dye complex layer. This layer would prevent the excited electrons moving from dye to ZnO nanocomposite [18]. Therefore, sensitization time increase apparently decreases the overall efficiency (η) of the DSSC.

From the Table 1. we could find that the best photoelectric parameters produced only at the two hours dye sensitization process and the short circuit current density (J_{sc}), open circuit voltage (V_{oc}), fill factor (FF) and efficiency (η) for the ZnO/MWCNT nanocomposite have been found as 11.85 mA/cm^2, 0.48 V, 48.76 % and 2.77 %, respectively.

3.3. UV- vis spectra

Figure 2 shows the UV-visible spectra of desorbed N719 dye from the ZnO and ZnO/MWCNT nanocomposite film. Here the UV-vis spectrum show the characteristics peaks of N719 dye around 375 and 500 nm [19]. Increase in the characteristic peaks of N719 dye with respect to the increasing concentrations of MWCNTs clearly depicts that the dye absorption property of this composite film. This results validates the improvement in the dye absorption with respect to the increasing concentrations of MWCNTs, respectively.

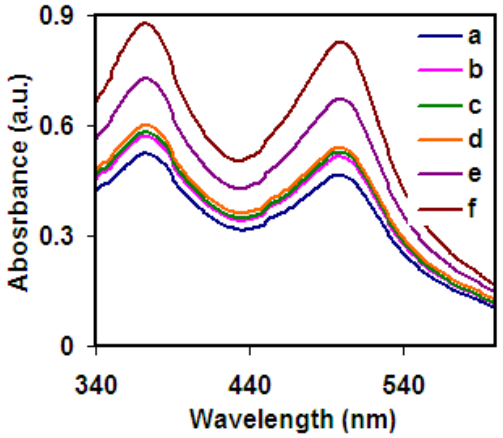

Figure 2. UV-vis spectra of desorbed N719 dye from ZnO and ZnO/MWCNT composite films containing a) 0 wt%, b) 0.1 wt%, c) 0.2 wt%, d) 0.3 wt%, e) 0.4 wt% and f) 0.5 wt% MWCNT.

3.4. Morphological characterization

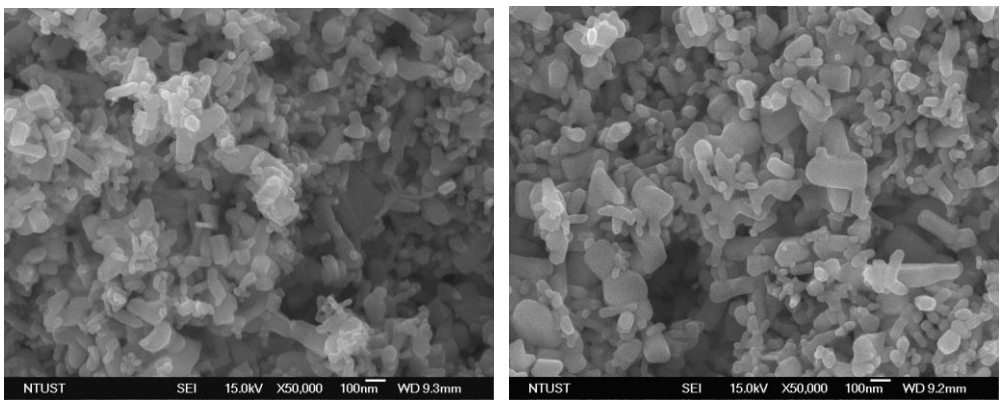

Figure 3. FESEM images of a) ZnO and b) ZnO/MWCNT composite films

Figure 3 shows FESEM images of the annealed porous nanocrystalline ZnO film (particle size <100 nm) and Figure. 3b shows annealed nanostructured ZnO/MWCNT composite film (0.3 wt.%) with reduced particle size and uniformed size distribution. The films were porous with an open structure and large pores with a diameter of around 50 nm. This shows the excellent connectivity between ZnO and MWCNTs in the composite film. Furthermore the composite show a well dispersed and embedded MWCNTs in the ZnO matrix.

3.5. Photovoltaic characterization

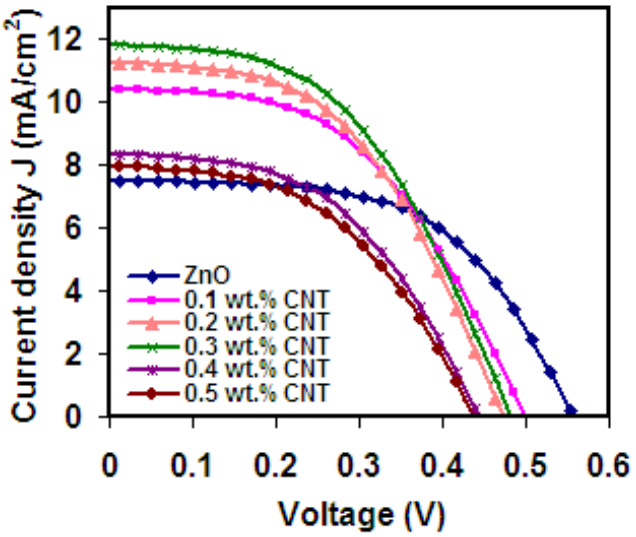

Figure 4. J–V characteristics of ZnO/MWCNT composite DSSCs containing a) 0 wt%, b) 0.1 wt%, c) 0.2 wt%, d) 0.3 wt%, e) 0.4 wt% and f) 0.5 wt% MWCNT.

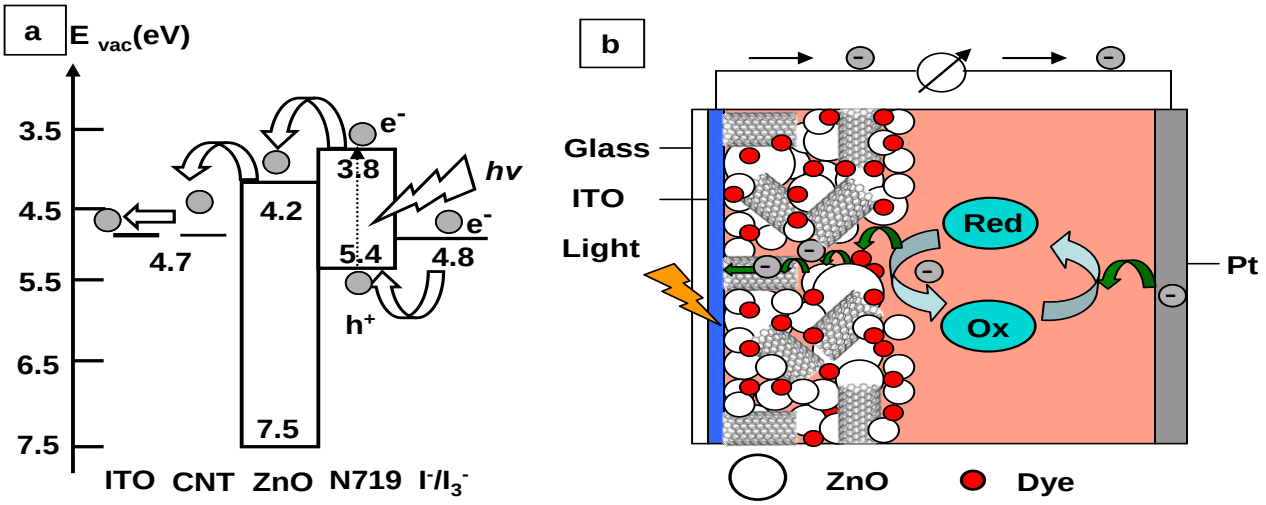

Figure 5. a) Schematic energy - level diagram and b) Proposed mechanism for the enhanced electron transport in the ZnO/MWCNT composite DSSC.

Figure 4 shows the J-V characteristic studies of ZnO and ZnO/MWCNT nanocomposite DSSCs. Here the J-V study results of ZnO and ZnO/MWCNT clearly indicate the photoelectric conversion efficiencies (η) of ZnO/MWCNT composite DSSCs are solely depends on MWCNT loadings in the electrodes. For the lower concentrations of MWCNTs, the DSSC efficiency increases upto 0.3 wt%, while for the higher concentrations of MWCNTs (> 0.3 %) the DSSCs efficiency were clearly decreasing.

Table 2. J–V characteristics of DSSCs based on ZnO/MWCNT composite films with various concentration of MWCNT.

Concentration of MWCNT (wt.%)	J_{sc} (mA/cm^2)	V_{oc} (V)	FF (%)	η (%)
0	7.48	0.55	57.02	2.37
0.1	10.42	0.49	49.34	2.56
0.2	11.28	0.47	49.38	2.62
0.3	11.85	0.48	48.76	2.77
0.4	8.39	0.44	49.07	1.83
0.5	7.99	0.43	48.50	1.70

Table. 2 shows the J–V characteristic study parameters of DSSCs based on ZnO and ZnO/MWCNT nanocomposite films with various concentration of MWCNTs. The ZnO/MWCNT nanocomposite film shows a short circuit current density (J_{sc}) of 11.85 mA/cm^2, open circuit voltage (V_{oc}) of 0.48 V, fill factor (FF) of 48.76% and the higher efficiency (η) of 2.77% for 0.3 wt% of MWCNT. Here the enhanced J_{sc} (from 7.48 to 11.85 mA/cm^2) is ascribed to the enhancement of collection and transport of electrons thereby reducing electron recombination and extending the electron life time in MWCNT composite film [20]. This is because at lower concentrations the MWCNT (upto 0.3 %) enhances the transport of electrons from the films to ITO substrates. At the same time, for the higher concentrations of MWCNT in the composite, it shields the penetration of light source on the anode surface, respectively. Furthermore, Figure. 5a shows the energy level diagram of individual components in the ZnO/MWCNT nanocomposite cells and Figure. 5b explains the efficient electron transport pathway through MWCNT, which enhance the transport of electrons from the film to ITO substrate, respectively.

3.6. Impedance analysis

Electrochemical impedance spectroscopy (EIS) has been widely used to investigate electronic and ionic reaction in DSSCs. The EIS response in high-frequency region is due to the charge transfer at counter electrode while the intermediate frequency response is attributed to ZnO/dye/electrode interface. The low frequency region is responsible for the diffusion in the electrolyte [21]. The EIS Nyquist and Bode plots for the DSSCs based on ZnO and ZnO/MWCNT(0.3 wt%) nanocomposite are shown in Figure. 6a and b. Here the first and second semicircles correspond to the charge transfer at the counter electrode (R_{ct1}) and at the ZnO/dye/electrolyte (R_{ct2}) respectively.

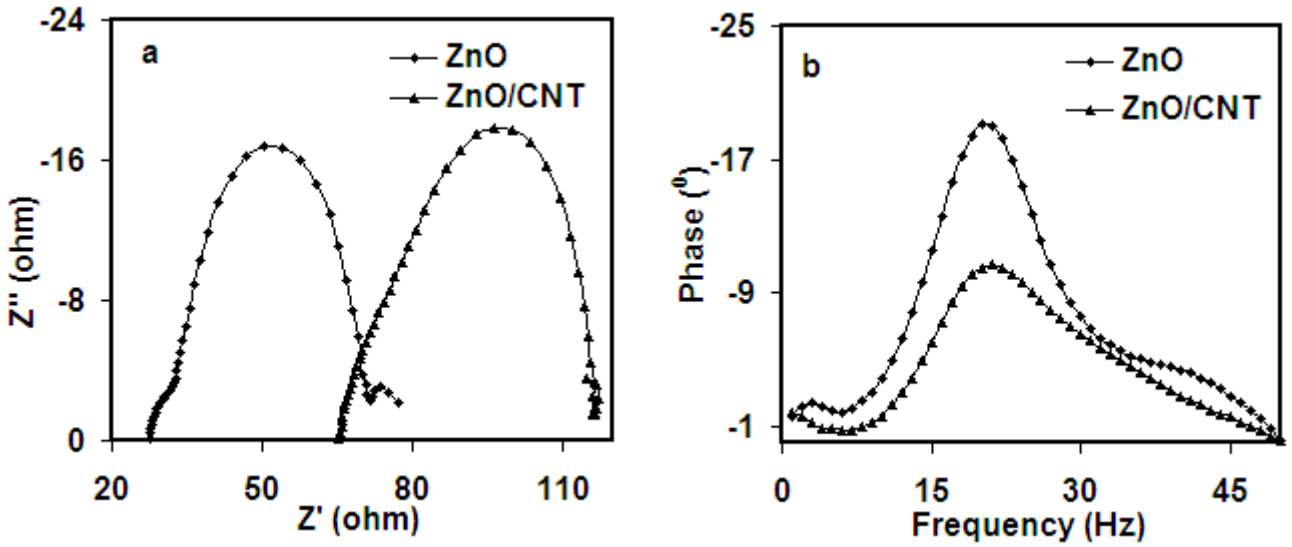

Figure 6. EIS spectra of ZnO and ZnO/MWCNT cells, a) Nyquist plots and b) Bode phase plots

Comparing to bare ZnO, the charge transport resistance (R_{ct2}) at the ZnO/MWCNT/dye/electrolyte interface is reduced from 134 Ω to 58 Ω. But the serial resistance (R_S) is increased from 22 Ω to 48 Ω. Using the formula $\tau_e = 1/2\pi f_{max}$ [21], the electron lifetime (τ_e) is estimated to be 8.39 ms for the ZnO cell while 14.92 ms for the ZnO/MWCNT cell. Here the longer τ_e for the ZnO/MWCNT clearly indicate that the reduced electron recombination which helps to enhance the overall cell efficiency [22]. This happens because the presence of optimized concentration of MWCNTs which favors the interfacial electron transfer and separates the electron hole pairs at the MWCNTs/ZnO interface [20]. Furthermore, to evaluate the performance of MWCNT with the other carbon based materials the ZnO/graphene and ZnO/fullerene nanocomposite films were prepared and tested under the same experimental conditions. Table 3 show the photoelectric parameters obtained for the ZnO/graphene and ZnO/fullerene nanocomposite DSSCs. Here the efficiency of ZnO/MWCNT nanocomposite film is higher than the ZnO/graphene and ZnO/fullerene nanocomposite films. However, ZnO/Graphene based nanocomposite exhibits higher fill factor and ZnO/Fullerene possess the higher V_{oc}, respectively.

Table 3. Comparison of J–V characteristics of the DSSCs of composite films of nanostructured carbon materials with ZnO.

Samples	J_{sc} (mA/cm^2)	V_{oc} (V)	FF (%)	η (%)
ZnO	7.48	0.55	57.02	2.37
MWCNT	11.85	0.48	48.76	2.77
Fullerene, C_{60}	8.56	0.51	51.93	2.28
Graphene	8.40	0.49	52.04	2.16

4. CONCLUSIONS

DSSCs based on ZnO/MWCNT nanocomposite films are fabricated by a direct mechanical mixing and spin coating method. The ZnO/MWCNT nanocomposite films with low loadings (<0.3 wt%) show enhanced J_{sc} and efficiency as compared with pristine ZnO cells. On the other hand, high MWCNT loadings (>0.3 wt%) resulted decrease in the efficiency. Under optimal conditions, the efficiency of ZnO/MWCNT (0.3 wt%) solar cell is 2.77%, which is higher than that of pure ZnO cell (2.37%). The improvement in the conversion efficiency is due to the fact that MWCNT reduce the electrolyte/electrode interfacial resistance, the recombination and enhances the transport of electrons from the film to ITO substrate, respectively. Further, the increase in dye adsorption rate is due to the increased surface area (MWCNTs in ZnO) and improved inter connectivity between the ZnO and MWCNT are also the particular reasons for the enhancement in the J_{sc} and efficiency. At the same time, the decrease in the conversion efficiency at high MWCNT loadings (>0.3 wt%) is due to light harvesting competition between MWCNT and dye molecules, which influences the light adsorption of the dye-sensitizer and consequently reduces the efficiency, respectively.

ACKNOWLEDGEMENT
This research work was supported by National Science Council, Taiwan and India-Taiwan Science and Technology Cooperation programme, DST, India.

References

1. B.Q. Zhang, C.S. Dandeneau, X. Zhou, G. Cao, *Adv. Mater.* 21 (2009), 4087.
2. H. Tang, K. Prasad, R. Sanjines, P.E. Schmid, F. Levy, *J. Appl. Phys.* 75 (1994) 2042.
3. U. Ozgur, Y.I. Alivov, C. Liu, A. Teke, M.A. Reshchikov, S. Dogan, V. Avrutin, S.J. Cho, H. Morkoc, *J. Appl. Phys.* 98 (2005) 041301.
4. F. Xu, L. Sun, *Ener. Environ. Sci.* 4 (2011) 818.
5. M. H. Habibi, M. Mikhak, M. Zendehdel , M. Habibi, *Int. J. Electrochem. Sci*. 7 (2012) 6787.
6. D.M. Guldi, V. Sgobba, *Chem. Commun.* 47 (2011) 606.
7. M.S. Mauter, M. Elimelech, *Environ. Sci. Tech.* 42 (2008) 5843.
8. L.J. Brennan, M.T. Byrne, M. Bari, Y.K. Guńko, *Adv. Energy Mater*. 1 (2011) 472.
9. T.H.Tsai, S.C. Chiou, S.M. Chen, *Int. J. Electrochem. Sci.* 6 (2011) 3333.
10. A.Kongkanand and P.V.Kamat, *ACS Nano* 1 (2007) 13.
11. Z. Peining, A.S. Nair, Y. Shengyuan, P. Shengjie, N.K. Elumalai, S. Ramakrishna, J. *Photochem. Photobiol. A: Chem.* 231 (2012) 9.
12. J. Yu, J. Fan, B. Cheng, *J. Power Sour. 196* (2011) 196, 7891.
13. S.L. Kim, S. Jang, R. Vittal, J. Lee, K. Kim, *J.Appl. Electrochem.* 36 (2006) 1433.
14. G. Zeng, K. Nian, K. Lee, *Diamond Relat. Mater.* 19 (2010) 1457.
15. D. Wei, H.E. Unalan, D. Han, Q. Zhang, L. Niu, G. Amaratunga, T. Ryhanen, *Nanotech*. 19 (2008) 4424006.
16. J. Liu, A.G. Rinzler, H. Dai, J.H. Hafner, R.K. Bradley, P.J. Boul, A. Lu, T. Iverson, K. Shelimov, C.B. Huffman, F. Rodriguez-Macias, Y.S. Shon, T.R. Lee, D.T. Colbert, R.E. Smalley, *Science* 280 (1998) 1253.
17. J. Chen, B. Li, J. Zheng, J. Zhao, Z. Zhu, *J. Phys. Chem. C* 116 (2012) 14848.
18. H. Horiuchi, R. Katoh, K. Hara, M. Yanagida, S. Murata, H. Arakawa, M. Tachiya, *J. Phys. Chem. B* 107 (2003) 2570.

19. J.J. Kim, K.S. Kim, G.Y. Jung, *J. Mater. Chem.*, 21 (2011) 7730.
20. J. Yu, T. Ma, S. Liu, *Phy. Chem. Chem. Phys.* 13 (2011) 3491.
21. R. Kern, R. Sastrawan, J. Ferber, R. Stangl, J. Luther, *Electrochim. Acta.* 47 (2002) 4213.
22. J. Bisquert, F. Fabregat-Santigo, I. Mora-Seró, G. Garcia-Belmonte, S. Giménez, *J. Phys. Chem. C* 113 (2009) 17278.